

# A Compatible Quadrilateral Finite Element for Plate Bending with Three-Nodal Degrees of Freedoms Each Node

S. Abo Diab

*This paper describes the formulation of a four node quadrilateral finite element for the use in the analysis of thin plate structures and the stiffened folded structures. The element has three degrees of freedom at each node, these are the displacement perpendicular to the plane of the plate and the two in-plane rotations. The element ensures conformity and inter-element continuity. Expressions for the displacement and rotations along the edges of the element are first formulated. Depending on these expressions, the approximation functions of the two in-plane rotations are derived. The state of the strain for the plate element is defined by the two rotations and it is not necessary to have an explicit formula of the displacement function in order to derive the element stiffness matrix. The derived element is fully compatible, when combined with plane strain element previously derived in the mid 80<sup>th</sup> and the classical beam elements for the analysis of stiffened folded plate structures.*

## 1 Introduction

A finite element approximation in the structural mechanics is usually evaluated upon criteria of a variational energy balance. The first energy balance used are the principle of minimum potential energy derived from the principle of virtual displacements or the principle of minimum complementary energy derived from the principle of virtual forces or their incremental forms. The finite element application based on such criteria requires conformity and inter-element continuity of the approximation functions for the displacements or the stresses between adjacent elements. The extended forms of these principles using the Lagrange multipliers method was applied in the early 70th of the last century, for a survey see e.g. (Washizu, 1982), (Pilkey and Wunderlich, 1994). The extended variational principle enables the continuity requirements to be relaxed. They allow also the displacement and the stresses to be selected independently. As a consequence, the desired minimum criterion is replaced by a stationary one. In (Atluri et al., 1983) is obviously declared that the origin of the hybrid mixed methods is related to earliest works of Pian in the early 60th. It also contains the state of development of the hybrid mixed methods until 1983. The pioneer work of (Pian, 1973) demonstrates the application of the hybrid mixed model. The basic idea of his formulation consists in selecting an independent frame functions for the displacement along the element boundaries which fulfill the continuity requirement between adjacent elements. For the stresses, approximation functions that fulfill a priori the equilibrium equations are chosen. This concept is inspired numerous researchers and still be used up to date in developing finite element for plate bending in order to overcome the so called  $c^1$ -continuity requirement of the displacement functions. The strategy of Pian is also adopted in some of research works represented by (Müller, 2006) in order to develop hybrid mixed plane stress and plate bending elements for solving the problems of linear and nonlinear statics and kinetics of folded plate structures. For solving the problems of the stiffened folded plate Structures the classical beam element with the cubic interpolation functions, a compatible plane stress element formulated using the same cubic functions (Müller and Abo Diab, 1987), (Müller et al., 1987), and a non-compatible thin plate bending element was used. Years later these works are presented internationally by (Müller et al., 1991, 1994). The compatibility issue of the thin plate bending element when joined to the other two mentioned elements at a folded plate edge was and still unsolved.

The plate bending problem is one of the most studied problems in the history of scientific research. It is classified under two main types, namely the thin Kirchhoff plate and the Mindlin thick plate. Recently an "in between" plate theory, the so called twist-Kirchhoff theory is generalized for arbitrary quadrilaterals and assessed for convergence by (Santos et. al, 2011).

A survey about the new development in the framework of the Mindlin plate can be found in (Senjanovic et al. 2014). There, the author reported that a comprehensive survey about both analytical and numerical solutions associated with thick (Mindlin) plate theories were worked out in (Liew and Kitipornchai, 1995). The governing equations of this theory for vibration analysis are also explained in details. Another survey about the recent developments of Mindlin-Reissner plate elements is presented by (Cen and Shang, 2015). In a finite element application based on the Mindlin plate theory the deflection and the two rotations are independently selected. For

this selection, only extended variational principles are suitable as a variational basis of a finite element approximation.

The equations, governing this problem can be found in the most text books of structural analysis (Timoshenko and Woinowsky-Krieger, 1987), (Reddy, 1984), (Ventsel and Krauthammer, 2001), (Zienkiewicz and Taylor, 2000), (Cook et al., 2001). The problem of developing finite elements with conforming shape functions is also discussed in details in addition to the previously listed books in many other text books about FEM (Akin, 2005); (Liu and Quek, 2005), (Felippa, 2017); (Rao, 2005). This paper does not aim to give a survey about finite elements for plate bending or to discuss the continuity requirements and conformity required by the application of the finite element method. It aims to introduce an idea to deal with finite element formulation for plate bending in a similar way as in applying a plane stress problem in what concerns the constructing of the approximation basis functions. So, the considered approximation basis functions are the in-plane rotations (like the Mindlin plate) rather than the displacement perpendicular to the plane of the plate. An explicit formula for the displacement inside the finite element is not necessary for deriving the stiffness matrix. The displacement is formulated along a finite element edge dependent on the degrees of freedoms of the nodes of that edge. As a result we get the classical Hermetian polynomials as an approximation functions (as derived by Pian), from which we can now derive the expression for the rotation along the edge. Now, depending on the expressions of the rotations at every two opposite edges of the element, the approximation basis functions for the rotation in the entire finite element are formulated. In such approximation procedure we can ensure compatibility requirements between the proposed plate bending element and the plane stress element as well as the beam elements, so that in a real building structure, where columns are firmly attached to the floor slabs, the columns will rotate about their axes by the same amount as the floor slabs. But this procedure has some disadvantage, in what concerns the evaluation of the external work of the element loading and the evaluation of the kinetic energy in which the explicit expression for the transverse displacement is necessary for developing the element load vector and the mass matrix. Some work must be further done to overcome such obstacles. Although, the nodal deflections and rotations of the element are computed, the deflection inside the finite element must be calculated by integrating the functions of rotations under preserving compatibility conditions. An approximate way for considering the external work and the kinetic energy consists in expanding the deflection at an arbitrary point inside the finite element as a multi variable Taylor series in the vicinity of the geometric center of the element. In the following the proposed procedure will be outlined in details. The state variables of the thin plate problem will be declared when mentioned, the equations governing the plate problem will be short outlined.

## 2 Formulation of the Governing Equations

Whenever is not pointed out, Latin indices range over the Cartesian co-ordinates, Greek indices range over the natural co-ordinates and indices between round brackets identify the nodal points. For example  $m^m$  ranges over  $x^i$  ( $i = 1,2$ ), where  $(m)$  denotes the number of the nodal points.

In the following, it is assumed that the assumptions of the Kirchhoff plate theory apply. The unknowns of the problem are the kinematic variables namely the deflection normal to the plane  $u_{x^3}^0(x^1, x^2)$ , the rotation about  $x^1$ -axes  $\varphi_{x^1}(x^1, x^2)$  and the rotation about  $x^2$ -axes  $\varphi_{x^2}(x^1, x^2)$  as well as the strain tensor with the components  $\varepsilon_{ij} = \{\varepsilon_{x^1x^1}, \varepsilon_{x^2x^1}, \varepsilon_{x^1x^2}, \varepsilon_{x^2x^2}\}$ . The other stress components vanish corresponding to the Kirchhoff assumptions. The two rotations will now be considered as primary unknowns and the deflection as secondary unknown.

The static variables are the stress tensor  $\sigma^{ij} = \{\sigma^{x^1x^1}, \sigma^{x^2x^1}, \sigma^{x^1x^2}, \sigma^{x^2x^2}\}$  as primary static unknowns. The additional shear stresses  $\{\sigma^{x^1x^3}, \sigma^{x^2x^3}\}$ , and the normal stress  $\sigma^{x^3x^3}$  are secondary static unknowns. That means, they could be calculated depending on the primary unknowns using equilibrium conditions and assuming a stress distribution over the plate thickness.

The stress tensor  $\sigma^{ij}$  is usually replaced by the moment tensor  $m^{ij} = \{m^{x^1x^1}, m^{x^2x^1}, m^{x^1x^2}, m^{x^2x^2}\}$  and the shear stresses  $\{\sigma^{x^1x^3}, \sigma^{x^2x^3}\}$  by the shear forces  $q^{x^1}, q^{x^2}$ . The moments and shear forces are measured per unit length.

Now, the equations governing the Kirchhoff plate will be recast depending on the primary unknowns.

The kinematic relation between the displacement at an arbitrary point of the plate thickness and the cross-sectional rotation assuming small displacement and neglecting the stretching are given by:

$$\begin{aligned} u_{x^1}(x^1, x^2, x^3) &= x^3 \varphi_{x^2}(x^1, x^2) \\ u_{x^2}(x^1, x^2, x^3) &= -x^3 \varphi_{x^1}(x^1, x^2) \\ u_{x^3}(x^1, x^2, x^3) &= u_{x^3}^0(x^1, x^2) \end{aligned} \quad (1)$$

Then, the strain displacement relations read

$$\begin{bmatrix} \varepsilon_{x^1 x^1} \\ \varepsilon_{x^2 x^1} \\ \varepsilon_{x^1 x^2} \\ \varepsilon_{x^2 x^2} \end{bmatrix} = -x^3 \begin{bmatrix} -\varphi_{x^2, x^1} \\ \varphi_{x^1, x^1} \\ -\varphi_{x^2, x^2} \\ \varphi_{x^1, x^2} \end{bmatrix} \quad (2)$$

The stress strain relations assuming linear elastic and isotropic material are given as follows:

$$\begin{bmatrix} \sigma_{x^1 x^1} \\ \sigma_{x^2 x^1} \\ \sigma_{x^1 x^2} \\ \sigma_{x^2 x^2} \end{bmatrix} = \frac{E}{(1-\nu^2)} \begin{bmatrix} 1 & 0 & 0 & \nu \\ 0 & (1-\nu)/2 & (1-\nu)/2 & 0 \\ 0 & (1-\nu)/2 & (1-\nu)/2 & 0 \\ \nu & 0 & 0 & 0 \end{bmatrix} \begin{bmatrix} \varepsilon_{x^1 x^1} \\ \varepsilon_{x^2 x^1} \\ \varepsilon_{x^1 x^2} \\ \varepsilon_{x^2 x^2} \end{bmatrix} \quad (3)$$

Replacing the stress components by the bending and twisting moments and making use of Eq. (2) yield:

$$\begin{bmatrix} m_{x^1 x^1} \\ m_{x^2 x^1} \\ m_{x^1 x^2} \\ m_{x^2 x^2} \end{bmatrix} = D \begin{bmatrix} 1 & 0 & 0 & \nu \\ 0 & (1-\nu)/2 & (1-\nu)/2 & 0 \\ 0 & (1-\nu)/2 & (1-\nu)/2 & 0 \\ \nu & 0 & 0 & 0 \end{bmatrix} \begin{bmatrix} -\varphi_{x^2, x^1} \\ \varphi_{x^1, x^1} \\ -\varphi_{x^2, x^2} \\ \varphi_{x^1, x^2} \end{bmatrix} \quad (4)$$

Where  $E$ ,  $\nu$  and  $h$  are the Young's modulus, Poisson's ratio and thickness, respectively.  $D = Eh^3/12(1-\nu^2)$  is the flexural rigidity.

The conditions of equilibrium at the differential plate element in the static analysis read:

$$\begin{aligned} m_{x^1 x^1, x^1} + m_{x^1 x^2, x^2} - q_{x^1} &= 0 \\ m_{x^2 x^1, x^1} + m_{x^2 x^2, x^2} - q_{x^2} &= 0 \\ q_{x^1, x^1} + q_{x^2, x^2} + \bar{q}_{x^3} &= 0 \end{aligned} \quad (5)$$

Separate considering the primary unknowns, show the similarity of the above presented problem to the plane stress problem. Since there is a system of ten algebraic and partial differential equations represented by two set of Eqns. (2), (3) and the first two relations of Eqn. (5) for determining the ten primary unknowns  $\varphi_i$ ,  $\varepsilon_{ij}$  and  $\sigma^{ij}$ . The additional static unknowns, the shear forces are linked to this system of equations through the third relation of Eqn. (5). This relation is a first order differential equation with two unknowns, in which the key for solving the Kirchhoff plate is hidden.

Substituting the shear forces from the first and second relation of Eqns. (5) in the third one give the higher order differential equation:

$$m_{x^1 x^1, x^1 x^1} + m_{x^2 x^1, x^2 x^1} + m_{x^1 x^2, x^1 x^2} + m_{x^2 x^2, x^2 x^2} + \bar{q}_{x^3} = 0 \quad (6)$$

The first differential equation governed the problem under consideration is obtainable by substituting Eqn. (4) into Eqn. (6) with the following result:

$$-\varphi_{x^2, x^2 x^2 x^1} - \varphi_{x^2, x^1 x^1 x^1} + \varphi_{x^1, x^2 x^2 x^2} + \varphi_{x^1, x^1 x^1 x^2} = \bar{q}_{x^3} / D \quad (7)$$

This equation is a third order differential equation with two unknowns.

The second differential equation results in from the Kirchhoff assumptions:

$$\begin{aligned}\varphi_{x^1}(x^1, x^2) &= u_{x^3, x^2}^0 \\ \varphi_{x^2}(x^1, x^2) &= -u_{x^3, x^1}^0\end{aligned}\quad (8)$$

With these assumptions, the in-plane displacements represented by Eqn. (1) are directly coupled with the transverse deflection. Furthermore, the assumption of vanishing the transverse shear strains  $\varepsilon_{x^1x^3}$ ,  $\varepsilon_{x^2x^3}$  is justified. This can be proved easily by substituting Eqn. (1) and (8) in the corresponding strain displacement relations. Eliminating the slopes of Eqn. (1) and (8) leads to the well-known differential equation of the Kirchhoff plate expressed only in terms of the deflections.

Eqns. (7) and (8) can also be considered as a Kirchhoff formulation of the problem provided that the two rotations are derivable from the same function (deflection). In other words the compatibility conditions associated with Eqn. (8) must apply.

The formulation in this way has the disadvantage that the additional kinematic unknown, the deflection  $u_{x^3}^0$  becomes an integral form of Eqn. (8).

Taking the derivative of the first relation of Eqn. (8) corresponding to  $x^1$  and the second one corresponding to  $x^2$  and summation gives the first order differential equation:

$$\varphi_{x^1, x^2} + \varphi_{x^2, x^1} = 0 \quad (9)$$

The last equation represents the divergence of the vector field  $\vec{\varphi} = \varphi_{x^1}\vec{e}^{x^1} + \varphi_{x^2}\vec{e}^{x^2}$ . This means that the Kirchhoff assumptions keep the vector sum of the rotations constant regardless of the vertical loading. The coupling between vertical loading and rotations follows through the derivatives in Eqn. (7).

It is interesting to observe that subtraction of the two mentioned equations instead of summation gives:

$$u_{x^3, x^1x^2}^0 = \frac{1}{2}(\varphi_{x^2, x^1} - \varphi_{x^1, x^2}) \quad (10)$$

The same relation is obtainable by formulation of the compatibility condition in terms of  $\varphi_i$  :

$$\frac{\partial^2 \varepsilon_{x^1x^1}}{(\partial x^1)^2} + \frac{\partial^2 \varepsilon_{x^2x^2}}{(\partial x^2)^2} = 2 \frac{\partial^2 \varepsilon_{x^1x^2}}{(\partial x^1 \partial x^2)} \quad (11)$$

This means, in a Kirchhoff plate the slopes couldn't be selected independently since Eqn. (9) or (10) must be observed. Therefore, the so called drilling degrees of freedoms  $u_{x^3, x^1x^2}^0(i)$  at element nodes are added in the literature in many finite element applications in order to construct compatible elements. This additional degrees of freedom cause the violation of the compatibility conditions with the mentioned plane stress element and the classical beam elements when joined at a folded plate edge and transformation difficulties at the corners. This path is not followed here, and the suggested element has only 3 DOFs at each node in favour of satisfying the compatibility at a folded plate edge.

The conditions of equilibrium at the differential plate element in the dynamic analysis neglecting the contribution of rotation inertia moments read:

$$\begin{aligned}m^{x^1x^1, x^1} + m^{x^1x^2, x^2} - q^{x^1} &= 0 \\ m^{x^2x^1, x^1} + m^{x^2x^2, x^2} - q^{x^2} &= 0 \\ q^{x^1, x^1} + q^{x^2, x^2} + \bar{q}^{x^3} - \rho \ddot{u}_{x^3}^0 &= 0\end{aligned}\quad (12)$$

The above discussion for the static case is also valid for the dynamic case. The differential equation (Eqn. 7) contain the additional term  $\rho \ddot{u}_{x^3}^0$ .

$$D(-\varphi_{x^2, x^2x^2x^1} - \varphi_{x^2, x^1x^1x^1} + \varphi_{x^1, x^2x^2x^2} + \varphi_{x^1, x^1x^1x^2}) + \rho \ddot{u}_{x^3}^0 = \bar{q}^{x^3} \quad (13)$$

The well-known Kirchhoff differential equation

$$\Delta \Delta D u_{x^3}^0 + \rho \ddot{u}_{x^3}^0 = \bar{q}^{x^3} \quad (14)$$

can be obtained by inserting Eqn. (8) into Eqn. (13).

Now, a brief description of the suggested finite element for plate bending follows.

### 3 Variational Approximation Basis

The current finite Element approximation is based on Hamilton's Principle. The 2D expression for the special case of the thin plate considered can be written in the absence of the prescribed boundary displacements in the following form:

$$\delta \int_{t_1}^{t_2} \left\{ \int_A \frac{1}{2} \chi_{ij} E^{ijkl} \chi_{kl} dA - \int_A \bar{q} u_{x^3}^0 dA - \frac{1}{2} \int_A \dot{u}_i \rho^{ij} \dot{u}_j dA - \sum_{i=1}^n \bar{F}^{(i)} u_{x^3}^0 \right\} dt = 0 \quad (15)$$

where

$t_1$  and  $t_2$  are two fixed time points of the vibration process,  $\delta$  is the first variation,  $E^{ijkl}$  is the tensor of the force-curvature dependency given in matrix form in Eqn. (4),  $A$  is the element area and  $dA$  its differential.  $\dot{u}_i$  is the velocity vector in which both displacement and rotation components are included,  $\rho^{ij}$  is the corresponding mass density matrix,  $\bar{F}^{(i)}$  is the concentrated load applied at the point  $(i)$ .

$\chi_{ij}$  is the curvature tensor, which reads expressed in terms of the primary unknowns  $\varphi_i$ :

$$\begin{bmatrix} \chi_{x^1 x^1} \\ \chi_{x^2 x^1} \\ \chi_{x^1 x^2} \\ \chi_{x^2 x^2} \end{bmatrix} = - \begin{bmatrix} -\varphi_{x^2, x^1} \\ \varphi_{x^1, x^1} \\ -\varphi_{x^2, x^2} \\ \varphi_{x^1, x^2} \end{bmatrix}_i \quad (16)$$

In Eqn. (15), the internal work associated with the bending and twisting moments is only considered.

### 4 Rotation Approximation Basis and Coordinate Systems

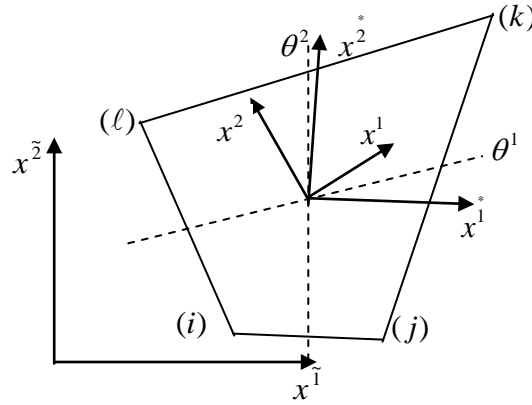


Figure 1: Thin plate element, with different coordinate systems

The plate finite element with the nodal points  $(i)$ ,  $(j)$ ,  $(k)$ ,  $(l)$  has three degrees of freedom each node. These are the displacement normal to the plate surface in  $x^3$ -direction and the two rotations about  $x^1$  and  $x^2$ -axes. The total number of degrees of freedom each element is then represented by the element nodal displacement vector with 12 degrees of freedom

$$\mathbf{u}_{n(n)} = \{ u_{x^3}^0(i), \varphi_{x^1}(i), \varphi_{x^2}(i), u_{x^3}^0(j), \varphi_{x^1}(j), \varphi_{x^2}(j), u_{x^3}^0(k), \varphi_{x^1}(k), \varphi_{x^2}(k), u_{x^3}^0(l), \varphi_{x^1}(l), \varphi_{x^2}(l) \} \quad (17)$$

Let the quadrilateral element be defined by its four nodal coordinates related to the global Cartesian coordinate system  $(x^1, x^2)$  as follows

$$x_{(p)}^i = \begin{bmatrix} x_{(1)}^1 & x_{(1)}^2 \\ x_{(2)}^1 & x_{(2)}^2 \\ x_{(3)}^1 & x_{(3)}^2 \\ x_{(4)}^1 & x_{(4)}^2 \end{bmatrix} \quad (18)$$

By mapping the quadrilateral element in a bi-unit square with the natural coordinate system  $(\theta^1, \theta^2)$ , the natural coordinates of the four element nodes are:

$$\theta_{(p)}^i = \begin{bmatrix} -1 & -1 \\ +1 & -1 \\ +1 & -1 \\ -1 & +1 \end{bmatrix} \quad (19)$$

Beside global Cartesian coordinate system  $(x^1, x^2)$ , parallel local coordinate system located at geometric center of the element  $(x^1, x^2)$  and the natural coordinate system  $(\theta^1, \theta^2)$ , a suitable Cartesian coordinate system  $(x^1, x^2)$  located at geometric center of the element is defined from the directions of the covariant base vectors and the perpendicular contra-variant base vectors computed in geometric center of the element. For more details see (Abo Diab, (2001, 2003)). Now the following differential geometry properties of the element are defined (Meißner, (1986), Klingbeil, (1989)):

\* Coordinates of an arbitrary point of the element

$$\begin{bmatrix} x^1 & x^2 \end{bmatrix} = \frac{1}{4} \begin{bmatrix} (1-\theta^1)(1-\theta^2) & (1+\theta^1)(1-\theta^2) & (1+\theta^1)(1+\theta^2) & (1-\theta^1)(1+\theta^2) \end{bmatrix} \begin{bmatrix} x_{(1)}^1 & x_{(1)}^2 \\ x_{(2)}^1 & x_{(2)}^2 \\ x_{(3)}^1 & x_{(3)}^2 \\ x_{(4)}^1 & x_{(4)}^2 \end{bmatrix} \quad (20)$$

\*The position vector of an arbitrary point of the element:

$$\vec{r} = x^i \bar{e}_i \quad (21)$$

\*Covariant basis vectors

$$\bar{g}_\alpha = \vec{r}_{,\alpha} = x^i_{,\alpha} \bar{e}_i \quad (22)$$

\*Derivatives of the covariant basis vectors

$$\bar{g}_{\alpha\beta} = \vec{r}_{,\alpha\beta} = x^i_{,\alpha\beta} \bar{e}_i \quad (23)$$

\*Metric coefficients

$$g_{\alpha\beta} = \bar{g}_\alpha \cdot \bar{g}_\beta = \vec{r}_{,\alpha} \cdot \vec{r}_{,\beta} = x^i_{,\alpha} \cdot x^j_{,\beta} \bar{e}_i \cdot \bar{e}_j \quad (24)$$

\*Contra-variant metric coefficients

$$g^{\alpha\beta} = (g_{\alpha\beta})^{-1} \quad (25)$$

\*Contra-variant basis vectors

$$\bar{g}^\alpha = g^{\alpha\beta} \cdot \bar{g}_\beta \quad (26)$$

\* Christoffel symbols

$$\Gamma_{\alpha\beta}^{\gamma} = g_{\alpha,\beta}^i \cdot g_i^{\gamma} \quad (27)$$

## 5 Formulation of the Finite Element Equations in the Natural Coordinate System

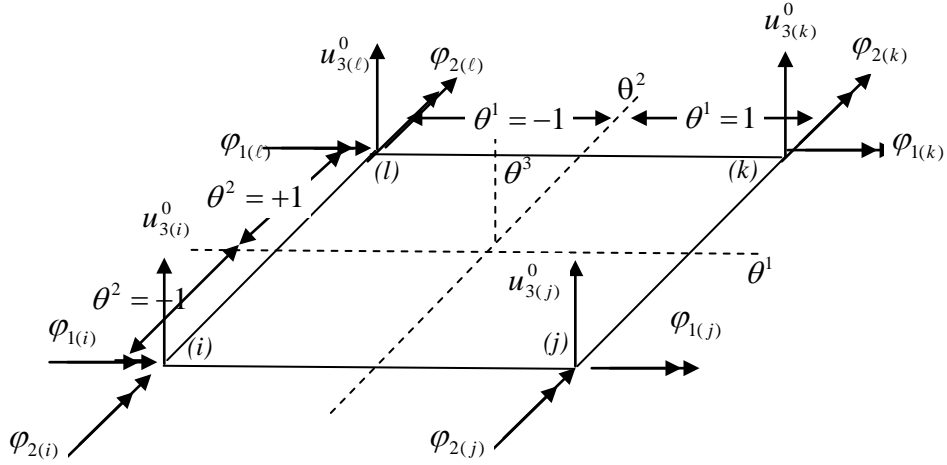


Figure 2. Bi-unit square, natural coordinate system, degrees of freedoms

It is convenient to construct the displacement approximation basis in the natural coordinate system. The element nodal displacement vector related to the natural coordinate system is as follow

$$\mathbf{u}_{n(n)} = \{ \mathbf{u}_{\theta^3(i)}^0, \phi_{1(i)}, \phi_{2(i)}, \mathbf{u}_{\theta^3(j)}^0, \phi_{1(j)}, \phi_{2(j)}, \mathbf{u}_{\theta^3(k)}^0, \phi_{1(k)}, \phi_{2(k)}, \mathbf{u}_{\theta^3(l)}^0, \phi_{1(l)}, \phi_{2(l)} \} \quad (28)$$

The displacements along the element boundary are approximated in terms of the classical Hermitian polynomials. From those displacements, the rotations are derived.

Arranging the approximation functions for the rotations along the four element boundaries gives the following relation

$$\begin{bmatrix} \phi_2^{(i)(j)} \\ \phi_1^{(j)(k)} \\ \phi_2^{(l)(k)} \\ \phi_1^{(i)(l)} \end{bmatrix} = \begin{bmatrix} -h_{1,1}^1 & 0 & -h_{2,1}^1 & -h_{3,1}^1 & 0 & -h_{4,1}^1 & 0 & 0 & 0 & 0 & 0 & 0 \\ 0 & 0 & 0 & h_{1,2}^2 & h_{2,2}^2 & 0 & h_{3,2}^2 & h_{4,2}^2 & 0 & 0 & 0 & 0 \\ 0 & 0 & 0 & 0 & 0 & 0 & -h_{3,1}^1 & 0 & -h_{4,1}^1 & -h_{1,1}^1 & 0 & -h_{2,1}^1 \\ h_{1,2}^2 & h_{2,2}^2 & 0 & 0 & 0 & 0 & 0 & 0 & 0 & h_{3,2}^2 & h_{4,2}^2 & 0 \end{bmatrix} \begin{bmatrix} \mathbf{u}_{\theta^3(i)}^0 \\ \phi_{1(i)} \\ \phi_{2(i)} \\ \mathbf{u}_{\theta^3(j)}^0 \\ \phi_{1(j)} \\ \phi_{2(j)} \\ \mathbf{u}_{\theta^3(k)}^0 \\ \phi_{1(k)} \\ \phi_{2(k)} \\ \mathbf{u}_{\theta^3(l)}^0 \\ \phi_{1(l)} \\ \phi_{2(l)} \end{bmatrix} \quad (29)$$

where

$$\begin{aligned}
h_1^1 &= \frac{1}{4} \left( 2 - 3\theta^1 + (\theta^1)^3 \right) \\
h_2^1 &= \frac{1}{4} \left( -1 + \theta^1 + (\theta^1)^2 - (\theta^1)^3 \right) \\
h_3^1 &= \frac{1}{4} \left( 2 + 3\theta^1 - (\theta^1)^3 \right) \\
h_4^1 &= \frac{1}{4} \left( 1 + \theta^1 - (\theta^1)^2 - (\theta^1)^3 \right)
\end{aligned} \tag{30}$$

and

$$\begin{aligned}
h_1^2 &= \frac{1}{4} \left( 2 - 3\theta^2 + (\theta^2)^3 \right); \\
h_2^2 &= \frac{1}{4} \left( 1 - \theta^2 - (\theta^2)^2 + (\theta^2)^3 \right) \\
h_3^2 &= \frac{1}{4} \left( 2 + 3\theta^2 - (\theta^2)^3 \right) \\
h_4^2 &= \frac{1}{4} \left( -1 - \theta^2 + (\theta^2)^2 + (\theta^2)^3 \right)
\end{aligned} \tag{31}$$

The notation  $\cdot_1$  denotes the derivative with respect to  $\theta^1$  and the notation  $\cdot_2$  denotes the derivative with respect to  $\theta^2$ .

The rotation  $\varphi_1(\theta^1, \theta^2)$  inside the finite element will be interpolated depending on the rotation of every two opposite element boundaries  $\varphi_1^{(j)(k)}(\theta^2)$ ,  $\varphi_1^{(i)(\ell)}(\theta^2)$  as follows

$$\varphi_1(\theta^1, \theta^2) = \frac{1}{2} (1 - \theta^1) \varphi_1^{(i)(\ell)} + \frac{1}{2} (1 + \theta^1) \varphi_1^{(j)(k)} \tag{32}$$

Similarly, the rotation  $\varphi_2(\theta^1, \theta^2)$  inside the finite element will be interpolated depending on the rotation of the other two opposite element boundaries  $\varphi_2^{(i)(j)}(\theta^1)$ ,  $\varphi_2^{(\ell)(k)}(\theta^1)$  as follows

$$\varphi_2(\theta^1, \theta^2) = \frac{1}{2} (1 - \theta^2) \varphi_2^{(i)(j)} + \frac{1}{2} (1 + \theta^2) \varphi_2^{(\ell)(k)} \tag{33}$$

Observing Eqn. (29) and Substituting into Eqns. (32) and (33) gives finally the following expression for the rotations

$$\begin{bmatrix} \varphi_1 \\ \varphi_2 \end{bmatrix} = \begin{bmatrix} h_1^{01} * h_{1,2}^2 & h_1^{01} * h_{2,2}^2 & 0 & h_2^{01} * h_{1,2}^2 & h_2^{01} * h_{2,2}^2 & 0 & h_1^{01} * h_{3,2}^2 & h_2^{01} * h_{4,2}^2 & 0 & h_1^{01} * h_{2,2}^2 & h_1^{01} * h_{2,2}^2 & 0 \\ -h_1^{02} * h_{1,1}^1 & 0 & -h_1^{02} * h_{2,1}^1 & -h_1^{02} * h_{3,1}^1 & 0 & -h_1^{02} * h_{4,1}^1 & -h_2^{02} * h_{3,1}^1 & 0 & -h_2^{02} * h_{4,1}^1 & -h_2^{02} * h_{1,1}^1 & 0 & -h_2^{02} * h_{2,1}^1 \end{bmatrix} \begin{bmatrix} u_{\theta^1(i)}^{\circ} \\ \varphi_{1(i)} \\ \varphi_{2(i)} \\ u_{\theta^1(j)}^{\circ} \\ \varphi_{1(j)} \\ \varphi_{2(j)} \\ u_{\theta^1(k)}^{\circ} \\ \varphi_{1(k)} \\ \varphi_{2(k)} \\ u_{\theta^1(\ell)}^{\circ} \\ \varphi_{1(\ell)} \\ \varphi_{2(\ell)} \end{bmatrix} \tag{34}$$

where

$$\begin{aligned}
h_1^{01} &= \frac{1}{2}(1-\theta^1) \quad ; \quad h_2^{01} = \frac{1}{2}(1+\theta^1) \\
h_1^{02} &= \frac{1}{2}(1-\theta^2) \quad ; \quad h_2^{02} = \frac{1}{2}(1+\theta^2)
\end{aligned} \tag{35}$$

The approximation basis functions (35) are sufficient for developing the element stiffness matrix. The shape functions constructed in this way satisfy the  $C^1$ -continuity requirement between adjacent plate elements and the compatibility requirement with the classical beam and the mentioned plane stress element when mixed at a folded plate edge. But they show what called stiffened corner rotation. The corners become stiff and a fine mesh size is required in order to avoid this over stiffness. Another way consists in introducing the drilling degrees of freedom.

## 6 Evaluating the Element Matrices in the Natural Coordinate System

Transforming the energy expression Eqn.(15) into the natural coordinate system leads to

$$\delta \int_{t_1}^{t_2} \left\{ \int_A \frac{1}{2} \chi_{\alpha\beta} E^{\alpha\beta\gamma\delta} \chi_{\gamma\delta} dA - \int_A \bar{q} u_{\theta^3}^0 dA - \frac{1}{2} \int_A \dot{u}_\alpha \rho^{\alpha\beta} \dot{u}_\beta dA - \sum_{i=1}^n \bar{F}^{(i)} u_{x^3}^0(i) \right\} dt = 0 \tag{36}$$

where

$$\chi_{\alpha\beta} = g_\alpha^i g_\beta^j \chi_{ij} \tag{37}$$

$$E^{\alpha\beta\gamma\delta} = g_i^\alpha g_j^\beta g_k^\gamma g_l^\delta E^{ijkl} \tag{38}$$

Applying the expressions of the rotations (Eqn. (34)) in the first term of Eqn.(36) yields the element stiffness matrix related to the natural coordinate system

$$k^{\lambda(m)\eta(n)} = \int_A N_{,\alpha\beta}^{\lambda(m)} E^{\alpha\beta\gamma\delta} N_{,\gamma\delta}^{\eta(n)} dA \tag{39}$$

$N_{,\alpha\beta}^{\lambda(m)}$  is a 4x12 matrix derived from the primary unknowns  $\varphi_\alpha$  corresponding to the following natural form of Eqn. (16).

$$\begin{bmatrix} \chi_{11} \\ \chi_{21} \\ \chi_{12} \\ \chi_{22} \end{bmatrix} = - \left\{ \begin{bmatrix} -\varphi_{2,1} \\ \varphi_{1,1} \\ -\varphi_{2,2} \\ \varphi_{1,2} \end{bmatrix}_i - \begin{bmatrix} \Gamma_{11}^1 & \Gamma_{11}^2 \\ \Gamma_{21}^1 & \Gamma_{21}^2 \\ \Gamma_{12}^1 & \Gamma_{12}^2 \\ \Gamma_{22}^1 & \Gamma_{22}^2 \end{bmatrix} \begin{bmatrix} -\varphi_2 \\ \varphi_1 \end{bmatrix} \right\} \tag{40}$$

The Christoffel symbols are defined in Eqn. (27).

Note that the integration of the element stiffness matrix can be performed depending on  $\varphi_\alpha$  only and there is no need to know the explicit expression of the deflection.

## 7 Considering the External Work and the Kinetic Energy

The explicit expression for the transverse displacement is necessary for developing the element load vector and the mass matrix. The following expansion of the deflection at any point  $(\theta^1, \theta^2)$  is the simplest approximation of the deflection depending on the element rotations

$$u_{\theta^3}^0(\theta^1, \theta^2) = u_{\theta^3}^0(0,0) + \frac{\partial u_{\theta^3}^0}{\partial \theta^1} \theta^1 + \frac{\partial u_{\theta^3}^0}{\partial \theta^2} \theta^2 \tag{41}$$

In Eqn. (41),  $u_{\theta^3}^0(0,0)$  is the deflection at the geometric center of the element where  $\theta^1 = 0, \theta^2 = 0$

When  $\theta^1, \theta^2$  are small enough, the previous expression represents the linear terms of the multi variable Taylor expansion of the deflection of the point  $(\theta^1, \theta^2)$  in the vicinity of the geometric center.

It is also possible to go higher in the approximation by involving the higher order terms of the Taylor expansion. For example, considering the second term of the Taylor series gives

$$u_{\theta^3}^0(\theta^1, \theta^2) = u_{\theta^3}^0(0,0) + \frac{\partial u_{\theta^3}^0}{\partial \theta^1} \theta^1 + \frac{\partial u_{\theta^3}^0}{\partial \theta^2} \theta^2 + \frac{1}{2!} \left( \frac{\partial^2 u_{\theta^3}^0}{(\partial \theta^1)^2} (\theta^1)^2 + \frac{\partial}{\partial \theta^1} \left( \frac{\partial u_{\theta^3}^0}{\partial \theta^2} \right) \theta^1 \theta^2 + \frac{\partial}{\partial \theta^2} \left( \frac{\partial u_{\theta^3}^0}{\partial \theta^1} \right) \theta^1 \theta^2 + \frac{\partial^2 u_{\theta^3}^0}{(\partial \theta^2)^2} (\theta^2)^2 \right) \quad (42)$$

Assuming an average value for the deflection of the geometric center depending on deflections of the four nodal points,

$$\left[ u_{\theta^3}^0(0,0) \right] = \begin{bmatrix} \frac{A_{(i)}}{A} & 0 & 0 & \frac{A_{(j)}}{A} & 0 & 0 & \frac{A_{(k)}}{A} & 0 & 0 & \frac{A_{(l)}}{A} & 0 & 0 \end{bmatrix} \begin{bmatrix} u_{\theta^3(i)}^{\circ} \\ \phi_{1(i)} \\ \phi_{2(i)} \\ u_{\theta^3(j)}^{\circ} \\ \phi_{1(j)} \\ \phi_{2(j)} \\ u_{\theta^3(k)}^{\circ} \\ \phi_{1(k)} \\ \phi_{2(k)} \\ u_{\theta^3(l)}^{\circ} \\ \phi_{1(l)} \\ \phi_{2(l)} \end{bmatrix} \quad (43)$$

then we can evaluate the element load vector and the mass matrix in the usual way.

$$m^{\lambda(m)\eta(n)} = \int_A N_i^{\lambda(m)} \rho^{ij} N_j^{\eta(n)} dA \quad (44)$$

where  $N_i^{\lambda(m)}$  is a 3x12 matrix obtained by arranging the deflection constructed corresponding to Eqn.(41) or Eq. (42) by making use of Eqns. (34), (43) and the two rotations presented in Eqn. (34).

$\rho^{ij}$  is the corresponding mass density matrix in which the displacements and rotations effects are included

$$\rho^{ij} = \begin{bmatrix} h & 0 & 0 \\ 0 & h^3/12 & 0 \\ 0 & 0 & h^3/12 \end{bmatrix} \quad (45)$$

In Eqn. (43), A is the element area and  $A_{(p)} ; (p)=(i),(j),(k),(l)$  is the subarea of the element included between the two element edges, which meet in (p), and the coordinate lines passing the geometric center.

The selection of the deflection in the explained form is kinematically justified. Eqn. (41) can be used to construct the shape functions for the secondary unknown dependent on the primary unknowns for linear cases and Eqn. (42) for nonlinear cases. By increasing the mesh refinement this selection represents a mathematic justified approximation for the deflection. Furthermore, in contrast to a Mindlin finite element application the deflection and the rotations are directly linked together.

The term of the equivalent nodal forces associated with the external work of the distributed load represented by the third term of Eqn. (36) is defined as follows:

$$\bar{f}^{\lambda(m)} = \int_A N^{\lambda(m)} \bar{N}_{(p)} \bar{q}^{(p)} dA \quad (46)$$

$\bar{N}_{(p)}$  are the shape functions that define the load function  $\bar{q}$  depended on its nodal values  $\bar{q}^{(p)}$ .

Applying the results of integrations from Eqn. (39), (43), (44) in the potential form Eqn. (35) leads to the following relation:

$$\delta \left( \frac{1}{2} u_{\lambda(m)} k^{\lambda(m)\eta(n)} u_{\eta(n)} + \frac{1}{2} \dot{u}_{\lambda(m)} m^{\lambda(m)\eta(n)} \dot{u}_{\eta(n)} - u_{\lambda(m)} \bar{f}^{\lambda(m)} \right) = 0 \quad (47)$$

All the element matrices are evaluated using the numerical integration.

Transformation to the local coordinate and after that to the global coordinate system leads to similar expressions. Finally, performing the variation leads to the following standard FEM-relation (in the absence of damping effects).

$$k^{m(m)n(n)} u_{n(n)} + m^{m(m)n(n)} \ddot{u}_{n(n)} = \bar{f}^{m(m)} \quad (48)$$

Note that the explicit formula of the deflection expressed in Eqns. (41), (42) is only used as secondary unknown in order to predict the distribution of the load and mass over the element nodes. It doesn't affect in any way the constructing of the stiffness matrix.

## 8 Numerical Examples

### 8.1 Square and Quadrilateral Clamped Plate

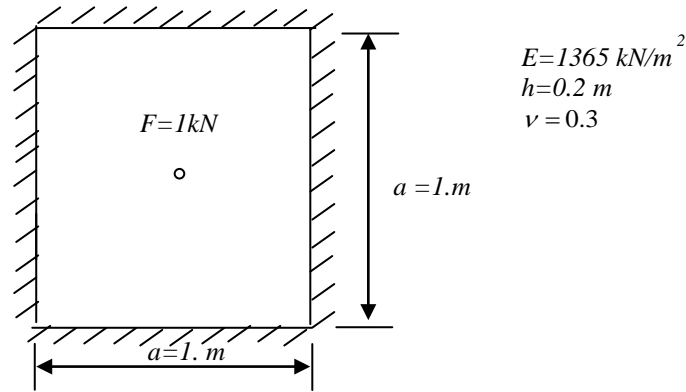


Figure 3: Clamped  $a \times a$  - thin plate, geometry, loads and material properties

The introduced shape functions of the plate element are verified numerically by solving a unit clamped square plate subjected to a central concentrated unit load and comparing the results with that provided by (Kikuchi, 1972). The elastic modulus  $E$ , the plate thickness  $h$  and Poisson's ratio  $\nu$  are chosen so that the flexural plate rigidity  $D$  is equal to unity. The results for the deflection and bending moment at the center of the plate as well as the edge moment at the plate edge are listed in Tab.1. The results are very close and the present solution is closer to the analytical solution for a coarse mesh. Therefore, the present FE-solution can be considered as a useful one.

Table 1: Clamped  $a \times a$  - square plate subjected to central concentrated load

| Mesh size                    | $u_{x^3}^0$ Center | $m^{x^1x^1}$ Center | $-m^{x^2x^2}$ Edge |
|------------------------------|--------------------|---------------------|--------------------|
| Mesh2x2                      | 0.00616371         | 0.02951631          | -0.07395867        |
| Mesh4x4                      | 0.00640053         | 0.02151799          | -0.05735057        |
| Mesh6x6                      | 0.00605365         | 0.02216200          | -0.05404186        |
| Mesh8x8                      | 0.00589296         | 0.02244994          | -0.05286639        |
| Mesh10x10                    | 0.00580687         | 0.02260017          | -0.05232305        |
| Mesh20x20                    | 0.00567175         | 0.02282372          | -0.05158771        |
| Mesh 10x10<br>(Kikuchi 1972) | 0.005731           | -                   | - 0.051 1          |

The clamped plate is computed again when subjected to uniformly distributed unit load. The results for different finite element mesh are depicted in Table 2. The results for the deflection and bending moment at the center of the plate as well as the edge moment at the plate edge are compared with that provided by (Taylor and Govindjee, 2002). Bearing in mind that the solution given in (Taylor and Govindjee, 2002) is an analytical one and obtained by solving a 2000 x 2000 system of equations, the present FE-solution can be considered also as a useful one.

Table 2: Clamped  $a \times a$  - square plate subjected to uniformly distributed load

| Mesh size                                | $u_{x^3}^0$ Center | $m^{x^1x^1}$ Center | $-m^{x^2x^2}$ Edge |
|--|--------------------|---------------------|--------------------|
| Mesh2x2                                  | 0.001540927022     | 0.0480769231        | -0.0369822485      |
| Mesh4x4                                  | 0.001459662935     | 0.0286914182        | -0.0484724170      |
| Mesh6x6                                  | 0.001358931589     | 0.0254405941        | -0.0501217006      |
| Mesh8x8                                  | 0.001319405506     | 0.0243294592        | -0.0506661992      |
| Mesh10x10                                | 0.001300319229     | 0.0238148708        | -0.0509051989      |
| Mesh20x20                                | 0.001274195602     | 0.0231318628        | -0.0512245695      |
| Analytical, Taylor and Govindjee, (2002) | 0.001265319087     | 0.02290508352       | -0.05131141375     |

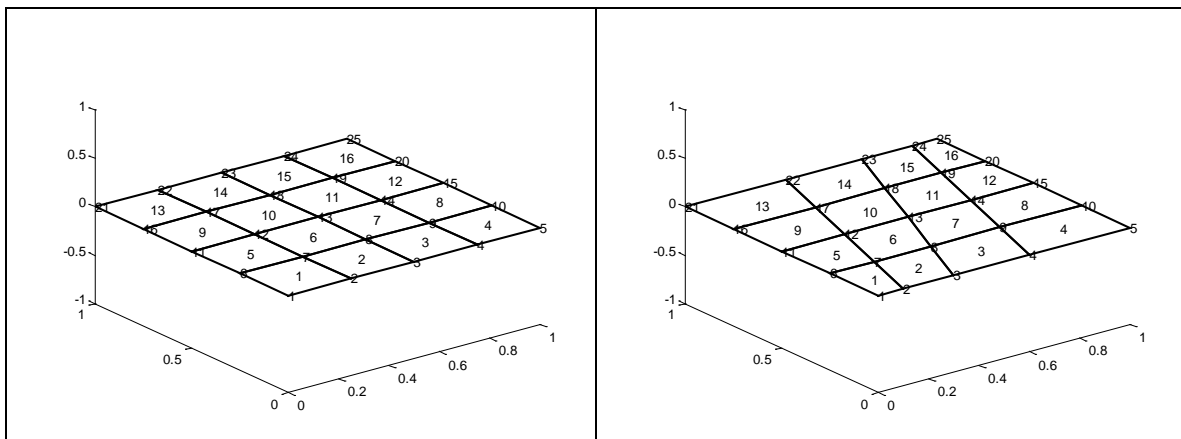
The free vibration analyses of the fully clamped square plate were carried out by using the present element. The mass density is chosen  $\rho = 5g/cm^3$  such that the factor  $\sqrt{D/\rho ha^4}$  is kept equal to unity. The plate is meshed by 20 x 20 finite elements. The first 40 non-dimensional natural frequencies are listed below in Tab.3. For a comparison purpose, a numerical solution obtained using a superposition method and a finite difference method in (Mochida, 2007), is also listed. In addition, other solution cataloged by (Leamy, 2016) is also given. Tab. 3 shows a good agreement between the three different solutions as well as a solution produced in (El-Gamel et al., 2016).

Table 3: Comparison of the non-dimensional natural frequencies  $\omega a^2 \sqrt{\rho h/D}$  using three different methods for a fully clamped square plate

| Order | non-dimensional natural frequencies | Leamy, (2016) | superposition method, Mochida (2007) |
|-------|-------------------------------------|---------------|--------------------------------------|
| 1.    | 35.857974                           | 35.09193      | 35.99                                |
| 2.    | 73.052083                           | 72.88823      | 73.39                                |
| 3.    | 73.052083                           |               | 73.39                                |
| 4.    | 107.058534                          | 107.4690      | 108.2                                |
| 5.    | 130.973867                          |               | 131.6                                |
| 6.    | 131.647400                          | 131.6154      | 132.2                                |
| 7.    | 162.801520                          | 164.3789      | 165.0                                |
| 8.    | 162.801520                          |               | 165.0                                |
| 9.    | 209.722899                          | 210.3520      | 210.5                                |
| 10.   | 209.722899                          |               | 210.5                                |
| 11.   | 215.556136                          | 219.3245      | 220.0                                |
| 12.   | 238.741077                          |               |                                      |
| 13.   | 239.891161                          | 242.1844      | 242.2                                |
| 14.   | 289.217111                          |               |                                      |

|     |            |          |  |
|-----|------------|----------|--|
| 15. | 289.217111 | 295.6943 |  |
| 16. | 308.004651 | 308.9221 |  |
| 17. | 308.316316 |          |  |
| 18. | 336.174611 |          |  |
| 19. | 336.174611 | 340.2308 |  |
| 20. | 359.632614 |          |  |
| 21. | 382.751019 | 370.6585 |  |
| 22. | 384.201061 | 392.7866 |  |
| 23. | 426.768970 | 427.2750 |  |
| 24. | 426.768970 |          |  |
| 25. | 450.563150 |          |  |
| 26. | 450.563150 |          |  |
| 27. | 452.961870 | 458.2581 |  |
| 28. | 453.734628 | 466.6105 |  |
| 29. | 498.256655 |          |  |
| 30. | 498.256655 | 510.1766 |  |
| 31. | 537.796562 |          |  |
| 32. | 561.245113 |          |  |
| 33. | 562.962864 | 561.4708 |  |
| 34. | 565.775504 |          |  |
| 35. | 565.972449 | 565.3911 |  |
| 36. | 591.106364 | 583.1376 |  |
| 37. | 591.106364 |          |  |
| 38. | 633.154575 |          |  |
| 39. | 634.348847 |          |  |
| 40. | 645.499077 |          |  |

The influence of mesh distortion on the results is studied also with the aid of a clamped square plate subjected to Eigen value analysis. The plate is first meshed by 4×4 regular elements, and secondly by the highly distorted 4×4 quadrilateral elements shown in Fig. 4. Tab. 4 shows the result of the difference in the non-dimensional natural frequencies for the regular mesh compared to the distorted mesh. The current result is comparable with that produced by various known finite elements such as (Jirousek and Guex, 1986), (Sze and Chow, 1991), (MacNeal, 1982), (Batoz and Ben Tahhar, 1982).



a) Regular mesh

b) Distorted mesh

Figure 4: Clamped square plate meshed by 4×4 elements for studying the influence of mesh distortion.

Table 4: Difference in the non-dimensional natural frequencies for distorted mesh over the clamped square plate (Fig. 4b) compared to the regular mesh (Fig. 4a)

| mesh      | $f_1$     | $f_2$     | $f_3$     | $f_4$      | $f_5$      | $f_6$      |
|-----------|-----------|-----------|-----------|------------|------------|------------|
| distorted | 34.498092 | 72.050984 | 73.815761 | 104.155672 | 137.258046 | 139.606801 |
| regular   | 34.038765 | 71.326579 | 71.326579 | 98.040161  | 151.646901 | 159.811277 |

An arbitrary quadrilateral clamped plate (Figure 5) is also studied. The plate is meshed by different number of quadrilateral elements. The results of the first six non-dimensional natural frequencies  $(\omega a^2 / \pi^2) \sqrt{\rho h / D}$  using the proposed element for three different mesh sizes are listed below in Table 5.

The present solution can be compared favorably with that provided by (Dozio and Carrera, 2011) for thickness-to-length ratios ( $h/a=0.005, 0.01, 0.05$ ).

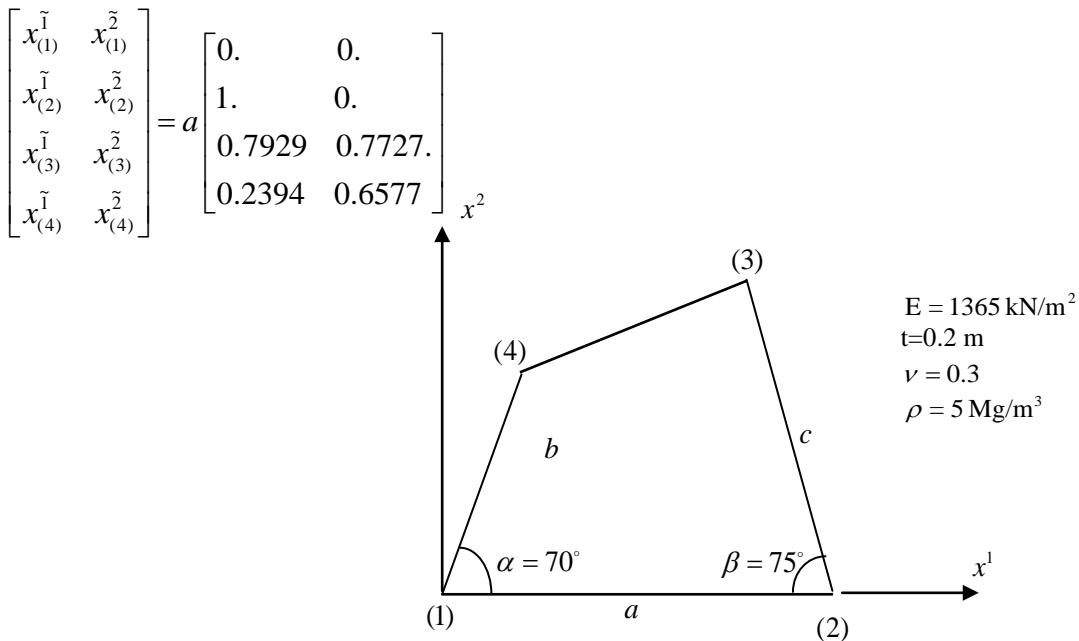


Figure 5: Clamped  $a \times a$  - thin plate, geometry, and material properties

Table 5: Comparison of the non-dimensional natural frequencies of clamped quadrilateral plate with the results provided in (Dozio and Carrera, 2011).

| mesh                      | $f_1$    | $f_2$     | $f_3$     | $f_4$     | $f_5$     | $f_6$     |
|---------------------------|----------|-----------|-----------|-----------|-----------|-----------|
| 2x2                       | 8.234961 | 11.329410 | 12.932349 |           |           |           |
| 4x4                       | 6.516769 | 12.481392 | 14.055341 | 18.910696 | 24.920696 | 27.287980 |
| 6x6                       | 6.648953 | 12.623712 | 14.021059 | 19.526633 | 21.653798 | 25.592772 |
| Dozio and Carrera, (2011) | 6.8294   | 13.115    | 14.319    | 20.777    | 22.296    | 25.627    |

## 8.2 Trapezoidal and Quadrilateral Cantilever Plate

Two cantilevered trapezoidal Plates with thickness  $h=0.2$ , unit plate-rigidity, Poisson ratio  $\nu = 0.3$  and mass density  $\rho = 5 Mg / m^3$  as shown in Fig. 6 are subjected to eigenvalue analysis. The results for the normalized

angular frequency  $\omega/\sqrt{D/\rho h a^4}$  for different element mesh size are listed in Table 6a and Table 6b. In both tables the results are obtained using element stiffness and mass matrices integrated numerically using a  $3 \times 3$ -point Gaussian rule. As may be seen, a very fast convergence is obtained. The first three digits do not change practically after the second mesh refinement. The solutions for the same plate models are reported in Korenev and Rabinovic (1980). They are close to the computed values and, also, obtained numerically using the Ritz-Method.

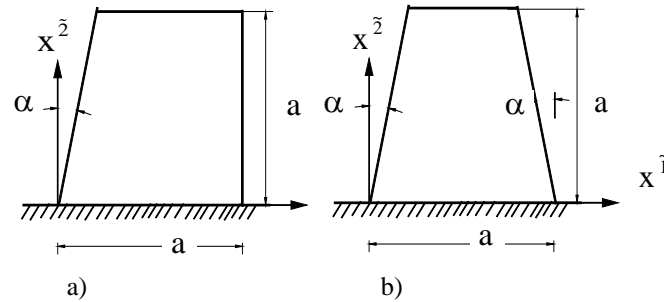


Figure 6: Cantilevered trapezoidal plate

Table 6a : Normalized angular frequency of cantilevered trapezoidal plate of Figure 6a

| Normalized angular frequency ( $\omega/\sqrt{D/\rho h a^4}$ ) |                    |                     |                     |                     |
|---|--------------------|---------------------|---------------------|---------------------|
| mesh  | $\alpha = 9^\circ$ | $\alpha = 18^\circ$ | $\alpha = 27^\circ$ | $\alpha = 36^\circ$ |
| 2x2   | 3.603188           | 3.774116            | 4.007905            | 4.420487            |
| 4x4   | 3.620411           | 3.801609            | 4.055401            | 4.518090            |
| 6x6   | 3.624900           | 3.809235            | 4.068422            | 4.543615            |
| Korenev and Rabinovic, (1980)                                 | 3.706              | 3.910               | 4.243               | 4.822               |

Table 6b: Normalized angular frequency of cantilevered trapezoidal plate of Figure 6b

| Normalized angular frequency ( $\omega/\sqrt{D/\rho h a^4}$ ) |                    |                     |                     |                     |
|---|--------------------|---------------------|---------------------|---------------------|
| mesh  | $\alpha = 6^\circ$ | $\alpha = 12^\circ$ | $\alpha = 18^\circ$ | $\alpha = 24^\circ$ |
| 2x2   | 3.674759           | 3.979360            | 4.462078            | 5.442542            |
| 4x4   | 3.694202           | 4.013026            | 4.525619            | 5.588472            |
| 6x6   | 3.699450           | 4.022966            | 4.545451            | 5.639143            |
| Korenev and Rabinovic (1980)                                  | 3.718              | 4.153               | 4.750               | 5.995               |

The last example is the general quadrilateral cantilever plate studied by (Dozio and Carrera, 2011) with side lengths  $a, b, c$  and internal angles  $\alpha = 60^\circ, \beta = 90^\circ$  and the geometrical properties given in Figure 7. The plate is subjected to Eigen value analysis for a different mesh size. The four vertices of the plate are defined by the following global Cartesian coordinates:

$$\begin{bmatrix} \tilde{x}_{(1)}^1 & \tilde{x}_{(1)}^2 \\ \tilde{x}_{(2)}^1 & \tilde{x}_{(2)}^2 \\ \tilde{x}_{(3)}^1 & \tilde{x}_{(3)}^2 \\ \tilde{x}_{(4)}^1 & \tilde{x}_{(4)}^2 \end{bmatrix} = a \begin{bmatrix} 0 & 0 \\ 1. & 0 \\ 1. & 1. \\ 0.433 & 0.75 \end{bmatrix}$$

The first six frequency parameters of the cantilever quadrilateral plate  $(\omega a^2 / \pi^2) \sqrt{\rho h / D}$  for different mesh size are listed in Tab. 7. For the one element structure the element stiffness and mass matrices are integrated exactly, for other mesh size, the integration is performed numerically using a  $3 \times 3$ -point Gaussian rule. The first line in the first cell is obtained by exact integration whereas the second line in the first cell is obtained using the numerical integration. For a comparison purpose, a numerical solution obtained using a variable kinematic Ritz method applied to free vibration analysis of arbitrary quadrilateral thin and thick isotropic plates in (Dozio and Carrera, 2011) is also listed.

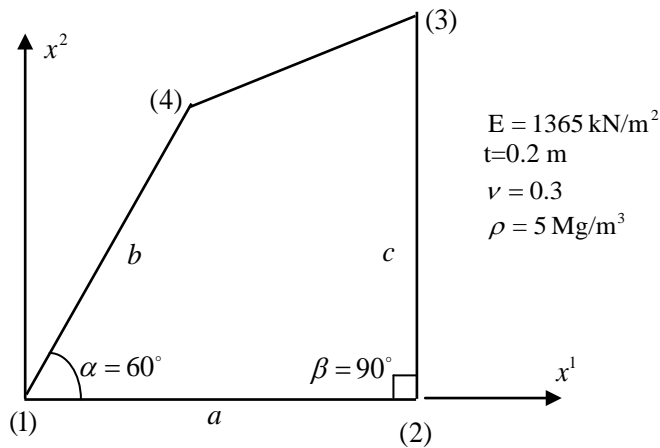


Figure 7: quadrilateral cantilever thin plate, geometry and material properties

Table 7: Comparison of the non-dimensional natural frequencies of cantilever quadrilateral plate with the results provided in (Dozio and Carrera, 2011).

| mesh                     | $f_1$    | $f_2$    | $f_3$    | $f_4$    | $f_5$    | $f_6$     |        |        |
|--------------------------|----------|----------|----------|----------|----------|-----------|--------|--------|
| one element              | 0.490913 | 0.985323 | 2.622993 | 4.074582 | 5.058621 | 10.508649 |        |        |
|                          | 0.491869 | 0.993002 | 2.940869 | 4.277306 | 6.117261 | 34.553542 |        |        |
| 2x2                      | 0.501838 | 1.596873 | 2.699458 | 4.134242 | 5.080273 | 6.210563  |        |        |
| 4x4                      | 0.507972 | 1.641754 | 2.825560 | 4.369777 | 6.380308 | 7.684967  |        |        |
| 6x6                      | 0.509355 | 1.655225 | 2.817862 | 4.385947 | 6.483664 | 7.676921  |        |        |
| Dozio and Carrera (2011) | 0.4857   | 1.3716   | 1.4692   | 2.2111   | 3.1421   | 3.3287    | 3.6373 | 4.5291 |

## 9 Conclusion

A compatible thin plate finite element with three degrees of freedoms at each node is presented. The element approximation basis makes use of the slopes rather than the deflection. The constructed approximation basis for the rotations is compatible and sufficient for developing the element stiffness matrix. For deriving the element load vector and the mass matrix the deflection at an arbitrary point inside the finite element is approximated as a multi variable Taylor expansion of the deflection in the vicinity of the geometric center of the element. The element developed is especially suitable for the use in analyzing stiffened folded structures since it ensures

compatibility requirements between the plate bending element, the plane stress element as well as the attached beam elements.

## References

- Abo Diab, S.: *Generalization of a reduced Trefftz-type approach*, in B. Möller, Hrsg., *Veröffentlichungen des Lehrstuhls für Statik.*, Technische Universität Dresden, Heft 4 (2001), Dresden (2001), p. 1-68.
- Abo Diab, S.: *Quadrilateral folded plate structure elements of reduced Trefftz type*, *CAMES*, vol. **10**: No. 4, (2003), p. 391-406.
- Akin, J. E., *Finite Element Analysis with Error Estimators - An Introduction to the FEM and Adaptive Error Analysis for Engineering Students*, Elsevier Butterworth-Heinemann, Amsterdam, ... Tokyo, (2005).
- Atluri, S. N.; Gallagher, R. H.; Zienkiewicz, O. C., eds., *Hybrid and mixed finite element method*, John Wiley & Sons, (1983).
- Batoz, L. J.; Ben Tahhar, M.: *Evaluation of a new quadrilateral thin plate bending element*, *Int. J. Num. Meth. in Engng.*, vol. 12: (1982), p. 1655-1677.
- Cen, S.; Shang Y.: *Developments of Mindlin-Reissner Plate Elements*, *Mathematical Problems in Engineering*, Hindawi Publishing Corporation, Volume 2015, (2015), Article ID 456740, 12 pages.
- Cook, R. D.; Malkus, D. S.; Plesha, M. E.; Witt, R. J.: *Concepts and applications of finite element analysis*, J. Wiley & Sons, Fourth edition, USA, (2001).
- El-Gamel, M.; Mohsen, A.; Abdrabou, A.: Sinc-Galerkin solution of the clamped plate eigenvalue problem, at: <https://www.researchgate.net/publication/303862644>, DOI: 10.1007/s40324-016-0086-9, (2016).
- Felippa, C. A.: Introduction to finite element methods, (ASEN 5007) Fall 2017, University of Colorado at Boulder, Department of Aerospace Engineering Sciences, USA, (2017).
- Jirousek, J.; Guex, L.: *The hybrid Trefftz finite element model and its application to plate bending*, *Int. J. Num. Meth. in Engng.*, vol. **23**: No. 4, (1986), p. 391-406.
- Kikuchi, F., Ando, Y.: Rectangular Finite Element for Plate Bending Analysis Based on Hellinger-Reissner's Variational Principle, *Journal of Nuclear Science and Technology*, 9:1, (1972), p. 28-35.
- Klingbeil, E., W.: *Tensorrechnung für Ingenieure*, BI Hochschultaschenbücher, Bd. 197, Wissenschaftsverlag, Mannheim, Wien, Zürich, (1989).
- Korenev, B. G.; Rabinovic, I. M.: *Baudynamik Handbuch*, Verlag für Bauwesen, Berlin, (1980).
- Leamy, M. J.: Semi-exact algebraic expressions for the natural frequencies of rectangular Kirchhoff-Love plates, *International Journal of Industrial Electronics and Electrical Engineering*, 4:2, (2016), p. 69-73.
- Liu, G. R.; Quek, S. S.: *The Finite Element Method A practical course*, Butterworth-Heinemann, Oxford, (2003).
- Macneal, R. H.: *Derivation of element stiffness matrix by assumed strain distributions*, *Int Nucl. Eng. Des.*, vol. 70: (1982), p. 3-12.
- Meißner, U. F., *Finite Elemente – Grundlagen für Flächentragwerke*, Kurs vII 1-15, Hannover, 19. Auflage, ws 85/86, Weiterbildendes Studium Bauingenieurwesen (1986).
- Mochida, Y.: Bounded Eigenvalues of Fully Clamped and Completely Free Rectangular Plates, A Thesis of Masters of Engineering In Mechanical Engineering, The University of Waikato, New Zealand, (2007).

- Müller, H.: Zur mechanischen Verhaltensanalyse von Tragwerken:STATRA-DGL, STATR-FEM Übersicht mit Beispielen, Publication Series of the Chair of Structural Design of TU Dresden, From research to practice in construction, Heft, Vol 6,(2006), Dresden. Germany.
- Müller, H.; Abo Diab, S.: Lineare Kinetik von stabversteiften Faltwerken mit FALT-FEM 5, Technische Universität Dresden, Sektion Grundlagen des Maschinenwesen Weiterbildungszentrum Festkörpermechanik, Konstruktion und rationeller Werkstoffeinsatz, Studentexte Stabtragwerke III, Heft 2/87, (Weißig), Dresden 1987,
- Müller, H.; Möller, B.; Hoffmann, A.; Abo Diab, S.: Faltwerksmechanik mit FALT-FEM- Kinetik und Stabilität sowie neuere Anwendungsfälle, *Bauplanung-Bautechnik*, Heft 1, Berlin, (1987), p. 30-33.
- Müller, H.; Hoffmann, A.; Möller, B.; Olden, J.; Abo Diab, S.: Einige Beispiele zum Einsatz gemischt-hybrider Elemente in FALT-FEM, In: In: Eibl, J., Obrecht, H., Wriggers, P. (eds.), *Finite Elements –Anwendung in der Baupraxis – Karlsruhe*, Ernst & Sohn,(1991), p. 319-330.
- Müller, H., Abo Diab, S., Graf, W., Hoffmann, A.: Lineare Kinetik von Faltwerken mit gemischt-hybriden Elementen, Internationaler Kongress über Anwendung der Mathematik in den Ingenieurwissenschaften (IKM), Weimar (1994), Berichtsband, p. 348-353.
- Pian, T. H. H.: *Finite element method by variational principle with relaxed continuity requirement in engineering, Proceedings international conference variational methods in engineering*, Vol. 1-3, Southampton, Uni. Press, England, (1973).
- Pilkey D. W., Wunderlich, W.: *Mechanics of structures variational and computational methods*, CRC Press, Boca Raton Ann Arbor London Tokyo, (1994).
- Rao, S. S.: *The Finite Element Method in Engineering*, Elsevier Butterwoth-Heinemann, Amsterdam,...,Tokyo, (2005).
- Reddy, J. N.: *Energy and variational methods in applied mechanics with an introduction to the finite element method*, J. Wiley & Sons, New York, Chichester, Brisbane, Toronto, Singapore, (1984).
- Santos, H.A.F.A ; Evans, J.A.; Hughes, T.J.R.: Generalization of the twist-Kirchhoff theory of plate elements to arbitrary quadrilaterals and assessment of convergence, ICES REPORT 11-25, The Institute for Computational Engineering and Sciences, The University of Texas at Austin, (2011).
- Sze, K. Y.; Chow, C. L.: *An efficient hybrid quadrilateral Kirchhoff plate bending element*, *Int. J. Num. Meth. in Engng.*, vol. 32: No. 4, (1991), p. 149-169.
- Taylor, L. R.; Govindjee, S., L. F. M.: Solution of Clamped Rectangular Plate Problems, Technical Report: UCB/SEMM-2002/09. Berkley, (2002).
- Timoshenko, S.; Woinowsky-Krieger, S.: *Theory of plates and shells*, McGraw-Hill Book Company, inc., second edition, New York, ..., Toronto, (1987).
- Ventsel, E.; Krauthammer, T.: *Thin Plates and Shells*, Theory, Analysis, and Applications, Marcel Dekker, Inc., New York, Basel, (2001).
- Washizu, K.: *Variational methods in elasticity and plasticity*, Pergamon Press, 3rd ed., Tokyo, (1982).
- Zienkiewicz, O. C., Taylor R. L.: *The finite element method*, fifth edition, volume 2. Solid Mechanics, Butterworth-Heinemann, Oxford, 2000.

---

Address: Sulaiman Abo Diab, Syria, Tartous, Hussain Al Baher  
email: sabodiab@tishreen.edu.sy or sabodiab@hotmail.com